Global atmospheric transport and source-receptor relationships for arsenic

Ka-Ming Wai[1], Shiliang Wu[2*], and Xueling Li[1]

[1]Dept. of Geological and Mining Engineering and Sciences, Michigan Technological University, Houghton, MI, USA

[2]Atmospheric Sciences Program, Dept. of Geological and Mining Engineering and Sciences and Dept. of Civil and Environmental Engineering, Michigan Technological University, Houghton, MI, USA

[*]e-mail: slwu@mtu.edu

Arsenic and many of its compounds are toxic pollutants in the global environment. They can be transported long distance in the atmosphere but the global source-receptor relationships between various regions have not been accessed yet. We develop the first global model for arsenic to better understand and quantify the inter-continental transport of arsenic. Our model reproduces the observed arsenic concentrations in surface air for various sites around the world. Our global arsenic emission inventory shows a global total anthropogenic arsenic emission of 21.4 Gg yr^{-1} and the global average atmospheric lifetime of arsenic is calculated to be of 5.1 days. Here we show that arsenic emissions from Asia and South America are the dominant sources for arsenic in the northern and southern hemisphere, respectively. Asian emissions are found to contribute to 53% and 41% of the total atmospheric arsenic deposition over Arctic and Northern America respectively. Another 32% of the atmospheric arsenic deposition to the Arctic region is attributed to European emissions. Our results indicate that reduction of anthropogenic arsenic emissions in Asia and South America can significantly reduce arsenic pollution not only locally but also globally.

Arsenic (As) is a chemical element ubiquitous in the global environment. Arsenic and many of its compounds have high toxicity and have been listed by the International Agency for Research on Cancer (IARC) as Group 1 carcinogens[1]. Recent studies[2,3] have shown levels of arsenic in rice in the United States significantly higher than the World Health Organization (WHO) standards for personal arsenic intake. The EU Directives has

set the new standard for annual mean atmospheric arsenic concentration of 6 ng m^{-3} effective from January, 2013.

Despite the toxicity of airborne arsenic, its measurements are relatively scarce compared to other heavy metals such as mercury and lead, especially in developing countries. Typical residence time of arsenic in the atmosphere is several days[4-6], making it capable of long-range transport. This implies that arsenic emissions from one region can significantly affect other regions downwind, but the global source-receptor relationship between various regions has not been quantified so far.

Sources of arsenic in the atmosphere include both anthropogenic and natural sources with dominant contributions from anthropogenic sources. Metal (copper, zinc and lead) smelting and coal combustion are two important anthropogenic arsenic sources[7-10] with copper smelting being the dominant source[6,8,9,10]. Additional minor anthropogenic sources include application of herbicide, wood preservation and waste incineration[10]. Natural sources of arsenic such as volcano activity, wind erosion and biological activity also contribute to arsenic in the atmosphere but are three times lower than those from anthropogenic sources[6,7].

Limited measurement data indicate that the range of concentrations can vary by several orders of magnitudes from less than 0.1 ng m^{-3} in remote sites to more than 10 ng m^{-3} in urban/industrial areas. In south polar atmosphere, the arsenic concentrations were reported to be less than 41 pg m^{-3} [11]. In China and Chile, the dominated arsenic source

56 regions in northern and southern hemisphere respectively, the arsenic concentrations were
57 reported to reach 15 ng m^{-3} or higher[12,13].
58
59 There have been some studies on the regional atmospheric transport of arsenic. Pacyna et
60 al.[14] and Akeredolu et al.[15] investigated the long-range transport of arsenic and other
61 heavy metals from Europe to Norway and the Arctic region, respectively. Gidhagen et
62 al.[12] studied the regional effects from smelter emissions of arsenic in Chile. Based on the
63 significant arsenic enrichment in snowpack samples from the Antarctic Plateau, Hong et
64 al.[16] proposed that the emissions of trace elements (including arsenic) from nonferrous
65 metal smelting and fossil fuel combustion processes in South America, especially in
66 Chile are the most likely sources.
67
68 In this study, we develop a global emission inventory for arsenic (more details in the
69 Methods section) and implement it into a global atmospheric chemical transport model.
70 The global arsenic model has been evaluated with available measurement data of
71 atmospheric arsenic concentrations around the world (Table 1 and Fig. 1). The model
72 results agree very well with the observations with high correlation (r^2 = 0.99). The global
73 total arsenic emission is calculated to be 21.4 Gg yr^{-1} with the breakdown for major
74 source regions summarized in Supplementary Information Table S1. We then apply the
75 global model to quantify the arsenic source-receptor relationships between various
76 regions.
77
78 The simulated results in Figure 1 reveal high arsenic concentrations over large areas in eastern
79 China and northern Chile, reaching 10 ng m^{-3} or higher, which are at least one order of magnitude

higher than those in the United States and Europe. Figure 1 also illustrates that the continental outflow of arsenic plumes from Asia is transported over the North Pacific towards North America following the Westerlies. Similarly the arsenic plumes from North America are transported across the North Atlantic to Europe. In the Southern Hemisphere, the major arsenic source is Chile. The arsenic plumes at lower latitudes are transported towards the tropical Pacific following the trade winds and those at higher latitudes are transported towards the Southern Atlantic following the Westerlies.

In order to better examine the source-receptor relationships between various regions, we carry out a suite of sensitivity simulations where arsenic emissions from a certain region is turned off in the model. For example, we shut off emissions from Asia in the sensitivity model run and then compare the calculated atmospheric arsenic concentrations (C_{no_Asia}) with those from the control run ($C_{control}$) to derive the percentage contribution of Asian emissions to atmospheric arsenic in the receptor region: $Contribution_{Asia} = (C_{control} - C_{no\_Asia}) / C_{control} \times 100\%$. Figure 2 shows the contribution of total (wet + dry) deposition for each continental-scale source. Similarly, the contribution of concentration for the corresponding source is shown in the Supplementary Information Fig. S1.

Arsenic emissions from Asia are found to make the dominant contributions to atmospheric arsenic concentration and deposition over the North Pacific Ocean (Fig. 2a). About 20-50% of atmospheric arsenic concentration and 20-80% of total arsenic deposition over the western part of Northern America are attributed to Asian emissions. Significant contributions to the Arctic region (up to 80% for atmospheric concentration

and up to 90% for total arsenic deposition) are also calculated for Asian emissions (Fig. 2a).

Figure 2b shows the contribution from European arsenic emissions. Besides Europe, the European contributions mainly extend northward to the Arctic and eastward over Russia in the Siberia region or to the north of Mongolia. The European emissions are also found to contribute to atmospheric arsenic over the northern Africa by up to 60%. Figure 2c shows the contribution from Northern American arsenic emissions. The eastward transport of the arsenic-laden plumes from Northern America leads to its large contribution to the North Atlantic Ocean (up to 80% right off the eastern coast of the US).

The average source-receptor relationships for atmospheric arsenic concentration and deposition between major regions in the Northern Hemisphere are summarized in Table 2. On average, about half of the total arsenic deposition over the Arctic region is attributed to Asian emissions, reflecting the strong arsenic emissions from Asia. The European emissions are calculated to contribute to about 30% of the total arsenic deposition to the Arctic. The Northern American contribution to arsenic in the Arctic (about 10%) is found to be much less than those from Asia or Europe, reflecting both the lower emission strengths and the lower latitudes of the sources. The Asian emissions are found to contribute to the total arsenic deposition in Northern America by 40%.

The contribution of arsenic emissions from South America is found to dominate over the Southern Hemisphere except for Southern Africa and Australia (Fig. 2d). More than 90%

126 of arsenic deposition over the Antarctic is attributed to emissions from South America,
127 which confirms the hypothesis by Hong et al.[16].
128
129 The inter-continental transport of arsenic, especially the significant global impacts
130 associated with arsenic emissions from certain source regions as shown by our results,
131 highlights the benefits of international cooperation to reduce arsenic pollution around the
132 world. These source-receptor relationships should be considered by researchers and
133 policy-makers in designing mitigation strategies for arsenic pollution.
134
135 **Methods**
136 **Model Description.** We develop a global arsenic model based on the GEOS-Chem
137 chemical transport model (http://geos-chem.org) v9-01-01. The GEOS-Chem model has
138 been applied to a wide range of researches related to tropospheric trace gases, aerosols,
139 and mercury[17-19]. It is driven by assimilated meteorological fields from NASA GMAO.
140
141 **Global Emissions Development.** Available data on arsenic emissions for various regions
142 around the world are compiled, processed and implemented in the model with a base year
143 of 1999. For Chile, the major arsenic source region in the southern hemisphere, we
144 follow Gidhagen et al.[12]. The Australian emissions are based on Australia's National
145 Pollutant Inventory (NPI) (http://www.npi.gov.au/resource/arsenic-and-compounds-0).
146 Arsenic emissions in the United States follow the U.S. EPA NATA (National-Scale Air
147 Toxics Assessment) inventory for 1999
148 (http://www.epa.gov/ttn/atw/nata1999/index.html). The Canadian emissions are based on

149 Environment Canada's National Pollutant Release Inventory (NPRI)
150 (http://www.ec.gc.ca/inrp-npri/). The European emissions of arsenic follow the
151 ESPREME inventory (http://espreme.ier.uni-stuttgart.de/).
152
153 There is no national emission inventory for arsenic available for China, so we develop the
154 inventory for China in this study. Arsenic emissions from the non-ferrous (copper, zinc
155 and lead) smelters are derived using the production data of non-ferrous metals from the
156 Statistical Yearbook[20] and the corresponding arsenic emission factors from Chilvers and
157 Peterson[10]. Arsenic emissions from coal-fired power plants in China follow Tian et al.[21].
158
159 Arsenic emissions from other countries around the world are estimated based on the
160 emissions of mercury (Hg), which is also a heavy metal but with better quantified
161 emission inventories. The As/Hg emission ratio is assumed to be 3.18, the same as the
162 ratio of median concentrations of As and Hg in rainwater samples[22,23].
163
164 The absolute majority (95%) of atmospheric arsenic sorbs onto aerosols[8], so we treat the
165 deposition processes of arsenic similarly as aerosols. The wet deposition of arsenic
166 follows the schemes used by Liu et al.[24] which considers the scavenging from convective
167 updrafts, rainout from convective anvils, and rainout and washout from large-scale
168 precipitation. The dry deposition follows a resistance-in-series scheme[25], with the surface
169 resistances following the work of Zhang et al.[26]. The global total wet deposition and dry
170 deposition of arsenic is 17.5 Gg yr^{-1} and 3.9 Gg yr^{-1} respectively. The global total
171 atmospheric burden of arsenic is calculated to be 297 Mg leading to a global average

atmospheric lifetime for arsenic of 5.1 days. The calculated atmospheric lifetimes for arsenic range from 3.2 to 5.3 days for different regions around the world (Table S1), which are within the range (2.5 – 9 days) reported in the literature[4-6].

For model evaluation, we focus on atmospheric arsenic measurement data from nonurban sites given the coarse spatial resolution (4^o latitude x 5^o longitude) of the global model. We collect available measurement data from various regions around the world in the literature and compile them in Table 1. Data for sites in the United States and Europe are from the Interagency Monitoring of Protected Visual Environments (IMPROVE) and the European Monitoring and Evaluation Programme (EMEP) network, respectively.

Initial model evaluation reveals that the model can reproduce the observed atmospheric arsenic concentrations (Table 1) over various sites around the world except for East Asia, where we find a systematic low bias with model results by a factor around three for all the six sites (Fig. 3). The most likely cause for this model-data discrepancy is the under-estimation of arsenic emission factors[10] used in developing the arsenic emission inventories in China. We then scale up the arsenic emissions from China by a factor of 3 in the model and find very good agreement between model results and observational data (Fig. 1).

Acknowledgement

The authors thank the EMEP data providers for making the arsenic data available. This publication was made possible by a U.S. EPA grant (grant 83518901). Its contents are solely the responsibility of the grantee and do not necessarily represent the official views of the U.S. EPA. Further, U.S. EPA does not endorse the purchase of any commercial products or services mentioned in the publication. S.W. acknowledges support from the NSF (grant 1313755).

Author contributions

K.M.W. and S.W. designed the entire study and wrote the manuscript. K.M.W. developed the arsenic model based on standard GEOS-Chem model and did all model experiments and analysis of outputs. X.L. assisted the project with literature review and database preparation at the early stage of the project.

Competing financial interests

The authors declare no competing financial interests.

References

1. IARC (International Agency for Research on Cancer). IARC Monographs on the evaluation of carcinogenic risks to humans (2013) (Available at: http://monographs.iarc.fr/ENG/Classification/).
2. Consumer Reports. Arsenic in your food (2012) (Available at: http://www.consumerreports.org/cro/magazine/2012/11/arsenic-in-your-food/index.htm).
3. Davis, M. A. *et al.* Rice consumption and urinary arsenic concentrations in U.S. children. *Environ. Health Perspect.* **120**, 1418–1424 (2012).
4. Pacyna, J.M. in *Lead, Mercury, Cadmium and Arsenic in the Environment Ch.7 (eds. Hutchinson, T.C. & Meema, K.M.)* (John Wiley & Sons, Chichester, 1987).
5. DET - Department of the Environment, Transport and the Regions, Scottish Executive, The National Assembly for Wales. A review of arsenic in ambient air in the UK (2000) (Available at http://uk-air.defra.gov.uk/reports/empire/arsenic00/arsenic_97v.pdf).
6. Walsh, P. R., Duce, R. A. & Fasching, J. L. Considerations of the enrichment, sources, and flux of arsenic in the troposphere. *J. Geophys. Res.* **84**, 1719–1726 (1979).
7. WHO (World Health Organization). *Air Quality Guidelines Second Edition* (WHO Regional Office for Europe, Copenhagen, Denmark, 2000).
8. Matschullat, J. Arsenic in the geosphere—a review. *Sci. Total Environ.* **249**, 297–312 (2000).
9. *Brimblecombe, P.* Atmospheric arsenic. *Nature* **280**, 104-105 (1979).
10. Chilvers, D.C. & Peterson, P.J. in *Lead, Mercury, Cadmium and Arsenic in the Environment Ch.17 (eds. Hutchinson, T.C. & Meema, K.M.)* (John Wiley & Sons, Chichester, 1987).
11. Maenhaut, W., Zoller, W. H., Duce, R. A. & Hoffman, G. L. Concentration and size distribution of particulate trace elements in the south polar atmosphere. *J. Geophys. Res.* **84**, 2421–2431 (1979).
12. Gidhagen, L., Kahelin, H., Schmidt-Thomé, P. & Johansson, C. Anthropogenic and natural levels of arsenic in PM_{10} in Central and Northern Chile. *Atmos. Environ.* **36**, 3803-3817

(2002).

13. Li, C. *et al.* Concentrations and origins of atmospheric lead and other trace species at a rural site in northern China. *J. Geophys. Res.***115**, D00K23 (2010).

14. Pacyna, J. M., Bartonova, A., Cornille, P. & Maenhaut, W. Modelling of long-range transport of trace elements. A case study. *Atmos. Environ.* **23**, 107-114 (1989).

15. Akeredolu, F. A. *et al.* The flux of anthropogenic trace metals into the arctic from the mid-latitudes in 1979/80. *Atmos. Environ.* **28**, 1557-1572 (1994).

16. Hong, S. *et al.* Evidence of Global-Scale As, Mo, Sb, and Tl Atmospheric Pollution in the Antarctic Snow. *Environ. Sci. Tech.* **46**, 11550-11557 (2012).

17. Bey, I. *et al.* Global modeling of tropospheric chemistry with assimilated meteorology: Model description and evaluation. *J. Geophys. Res.* **106**, 23,073 – 23,095 (2001).

18. Martin, R.V. *et al.* Interpretation of TOMS observations of tropical tropospheric ozone with a global model and in-situ observations. *J. Geophys. Res.* **107**, 4351 (2002).

19. Huang, Y., Wu, S., Dubey, M. K. & French, N. H. F. Impact of aging mechanism on model simulated carbonaceous aerosols. *Atmos. Chem. Phys.* **13**, 6329–6343 (2013).

20. China Non-ferrous Metals Industry Association. *The Yearbook of Nonferrous Metals Industry of China 1999* (in Chinese, China Nonferrous Metals Industry Press, Beijing, 1999).

21. Tian, H. *et al.* Atmospheric emissions estimation of Hg, As, and Se from coal-fired power plants in China. *Sci. Total Environ.* **409**, 3078-3081 (2011).

22. Landing, W. M., Caffrey, J. M., Nolek, S. D., Gosnell, K. J. & Parker, W. C. Atmospheric wet deposition of mercury and other trace elements in Pensacola, Florida. *Atmos. Chem. Phys.* **10**, 4867-4877 (2010).

23. Galloway, J. N., Thornton, J. D., Norton, S.A., Volchok, H. L. & McLean, R. A. N. Trace metals in atmospheric deposition: A review and assessment. *Atmos. Environ.* **16**, 1677-1700 (1982).

24. Liu, H., Jacob, D. J., Bey, I. & Yantosca, R. M. Constraints from ^{210}Pb and ^{7}Be on wet

deposition and transport in a global three-dimensional chemical tracer model driven by assimilated meteorological fields. *J. Geophys. Res.* **106**, 12109-12128 (2001).

25. Wesely, M. L. Parameterization of surface resistances to gaseous dry deposition in regional-scale numerical-models. *Atmos. Environ.* **23**, 1293–1304 (1989).
26. Zhang, L. M., Gong, S. L., Padro, J. & Barrie, L. A size-segregated particle dry deposition scheme for an atmospheric aerosol module. *Atmos. Environ.* **35**, 549–560 (2001).
27. Chen, J. *et al.* Characteristics of trace elements and lead isotope ratios in $PM_{2.5}$ from four sites in Shanghai. *J. Hazard. Mat.* **156**, 36-43 (2008).
28. Yang, Y. *et al.* Elemental composition of $PM_{2.5}$ and PM_{10} at Mount Gongga in China during 2006. *Atmos. Res.* **93**, 801-810 (2009).
29. Kang, J. *et al.* A five-year observation of atmospheric metals on Ulleung Island in the East/Japan Sea: Temporal variability and source identification. *Atmos. Environ.* **45**, 4252-4262 (2011).
30. Kaneyasu, N. & Takada, H. Seasonal variations of sulfate, carbonaceous species (black carbon and polycyclic aromatic hydrocarbons), and trace elements in fine atmospheric aerosols collected at subtropical islands in the East China Sea. *J. Geophys. Res.* **109**, D06211 (2004).

Figure Legends

Figure 1 | Surface-level concentrations. Annual average arsenic concentrations measured at various stations (circles) overlaying on the computed concentrations (background).

Figure 2 | Contributions from difference regions. Percent contributions of arsenic total deposition from: (a) Asia; (b) Europe; (c) Northern America; and (d) South America.

Figure 3 | O**bserved and simulated concentrations over East Asia.** A comparison of arsenic concentrations between observation and simulation over East Asia before and after the adjustment of China emissions. The value of r^2 is shown for the data before the adjustment.

298

Table 1| Model simulated annual average surface atmospheric arsenic concentrations compared with observations.

Site	Model result (ng m^{-3})	Observations (ng m^{-3})	Year of observations	Source for observational data
Storhofdi, Iceland (63.4° N, 20.3° W)	0.06	0.08	1999	EMEP
Peyrusse Vieille, France (43.6° N, 0.2° E)	0.19	0.23	2003	EMEP
Neuglobsow, Germany (53.1° N, 13.0° E)	0.47	0.55	1999	EMEP
Topoliniky, Slovakia (48.0 ° N, 17.8° E)	0.35	0.38	2003	EMEP
Montseny, Spain (41.8° N, 2.4° E)	0.19	0.38	2003	EMEP
Bredkalen, Sweden (63.8° N, 15.3° E)	0.10	0.10	2002	EMEP
Pallas, Finland (61.0° N, 24.2° E)	0.30	0.22	2000	EMEP
Rucava, Latvia (56.2° N, 21.1° E)	0.58	0.61	2002	EMEP
Florida, US (30.1° N, 84.2	0.53	0.46	2001	IMPROVE

° W)				
Virginia, US (37.6° N, 79.5° W)	0.68	0.54	2000	IMPROVE
Maine, US (46.7° N, 68.0 ° W)	0.23	0.22	2001	IMPROVE
Michigan, US (47.5° N, 88.1° W)	0.33	0.27	1999	IMPROVE
South Dakota, US (43.7° N, 101.9° W)	0.11	0.09	1999	IMPROVE
Texas, US (31.8° N, 104.8 ° W)	0.38	0.40	1999	IMPROVE
Washington (46.6° N, 121.4° W)	0.11	0.08	2000	IMPROVE
California (34.2° N, 116.9 ° W)	0.17	0.16	1999	IMPROVE
Idaho (44.2° N, 114.9° W)	0.11	0.08	1999	IMPROVE
Hawaii, US (19.4° N, 155.3° W)	0.04	0.04	2001	IMPROVE
Alaska1, US (56.5° N, 132.8° W)	0.04	0.07	2004	IMPROVE
Alaska2, US (55.3° N,	0.04	0.04	2001	IMPROVE

160.5° W)				
Beijing, China (39.8° N, 117.0° W)	16.74	18.00	2005	[13]
Shanghai, China (31.4° N, 121.3° E)	26.75	27.00	2004-2005	[27]
Sichuan, China (29.6° N, 102.0° E)	3.80	6.10	2006	[28]
Ulleung Island, S. Korea (37.5° N, 130.9° E)	4.63	2.97	2003-2008	[29]
Amami-Oh-shima Island, Japan (28.5° N, 128.5° E)	0.71	1.00	1991-1994	[30]
Miyako-jima Island, Japan (24.5° N, 125.5° E)	1.23	0.70	1993-1994	[30]
Quillota, Chile (32.9° S, 71.2° W)	31.53	30.70	1999-2000	[12]
Quillagua, Chile (21.6° S, 69.5° W)	4.58	6.50	1999-2000	[12]

303

Table 2| Source-Receptor relationships for atmospheric arsenic concentration (deposition) between various regions*.

		Source regions		
		Asia	Europe	Northern America
Receptor regions	Arctic (70 – 90°N, 179°W – 179°E)	43.9 (52.6)	35.9 (31.5)	11.3 (9.5)
	Asia (10 – 70°N, 60 – 145°E)	69.5 (71.8)	15.6 (15.7)	0.8 (0.9)
	Europe (35 – 70°N, 5°W – 60°E)	6.4 (10.7)	78.8 (71.9)	2.2 (3.4)
	Northern America (30 – 70°N, 125 – 65°W)	27.1 (41.3)	2.5 (1.6)	68.8 (54.5)
	Western US (30 – 48°N, 125 – 100°W)	35.7 (52.9)	0.6 (0.7)	60.0 (41.3)
	Eastern US (30 – 48°N, 100 – 70°W)	8.0 (16.1)	0.3 (0.4)	91.0 (80.7)

*Shown as the percentage contribution to total atmospheric arsenic concentration (deposition) in the receptor region from the source region.

304

305

306

307

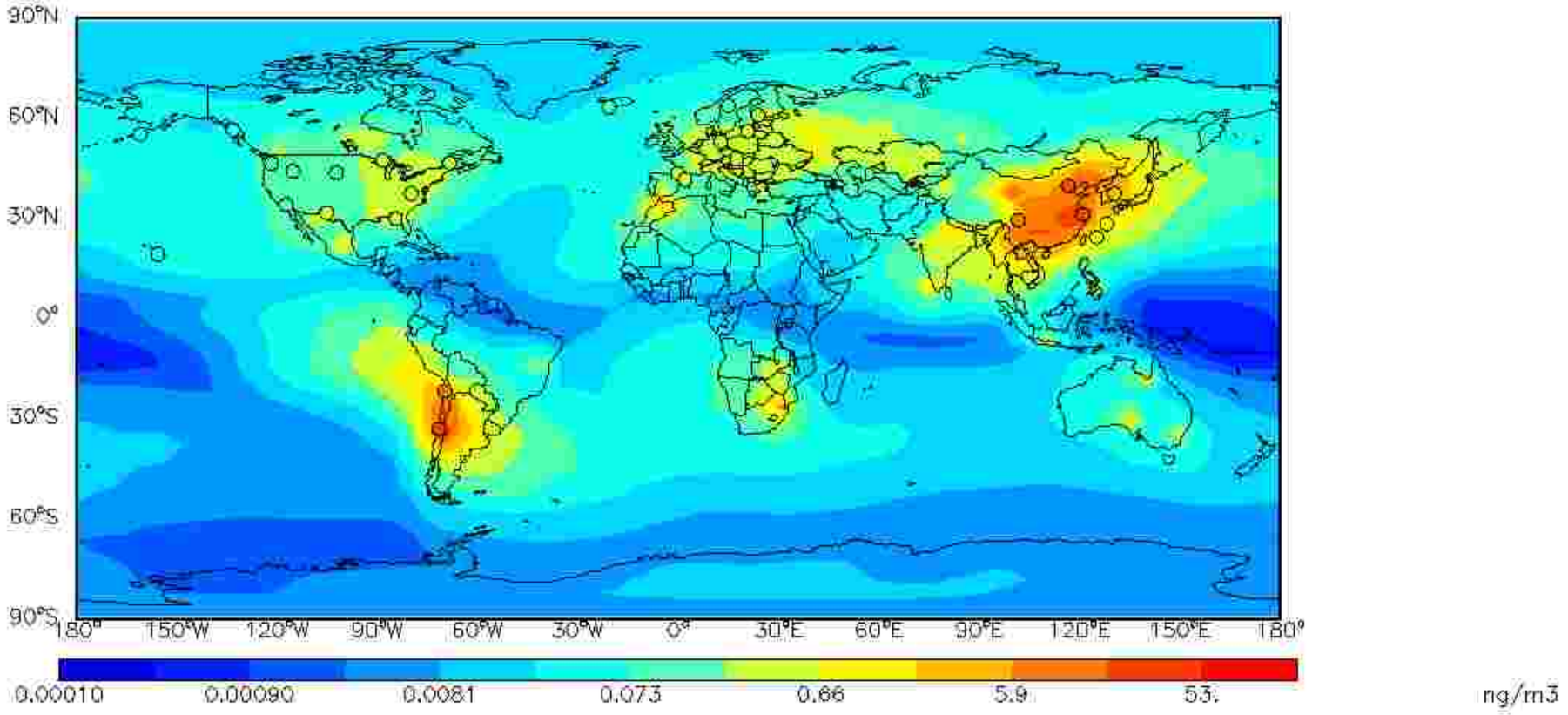
90°N
60°N
30°N
0°
30°S
60°S
90°S
180°
150°W
120°W
90°W
60°W
30°W
0°
30°E
60°E
90°E
120°E
150°E
180°
0.00010
0.00090
0.0081
0.073
0.66
5.9
53.
ng/m3

a)

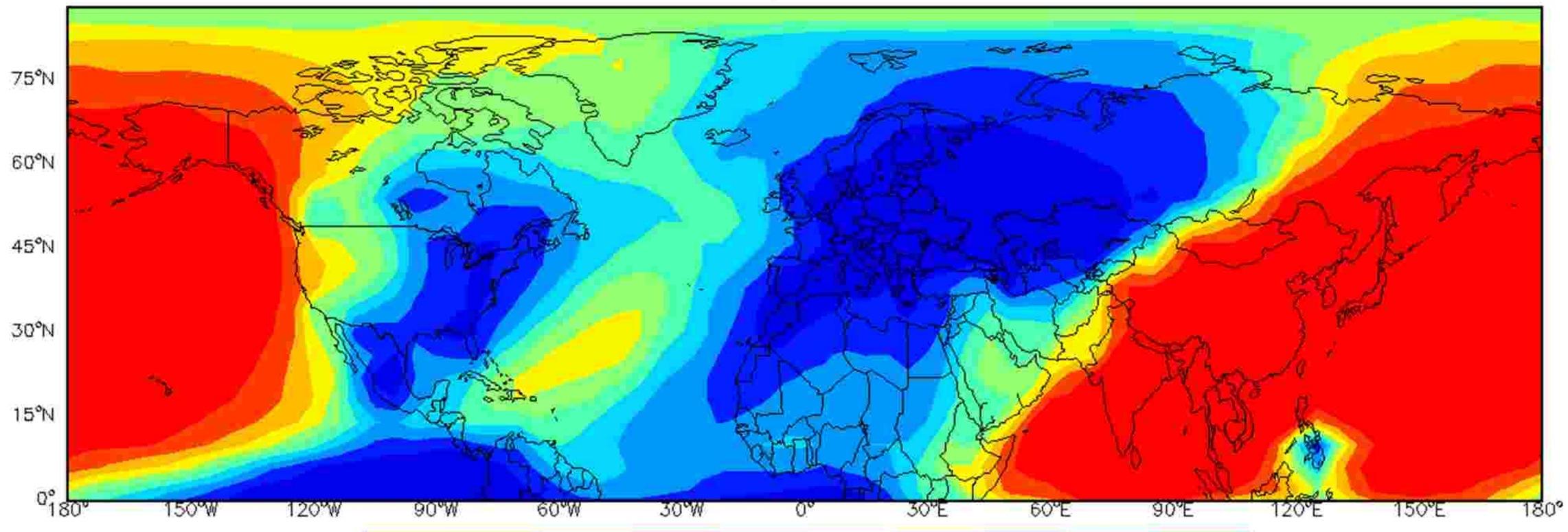
75°N
60°N
45°N
30°N
15°N
0°
180°
150°W
120°W
90°W
60°W
30°W
0°
30°E
60°E
90°E
120°E
150°E
180°
0.0
10.
20.
30.
40.
50.
60.
70.
80.
90.
1.0e+02
%

b)

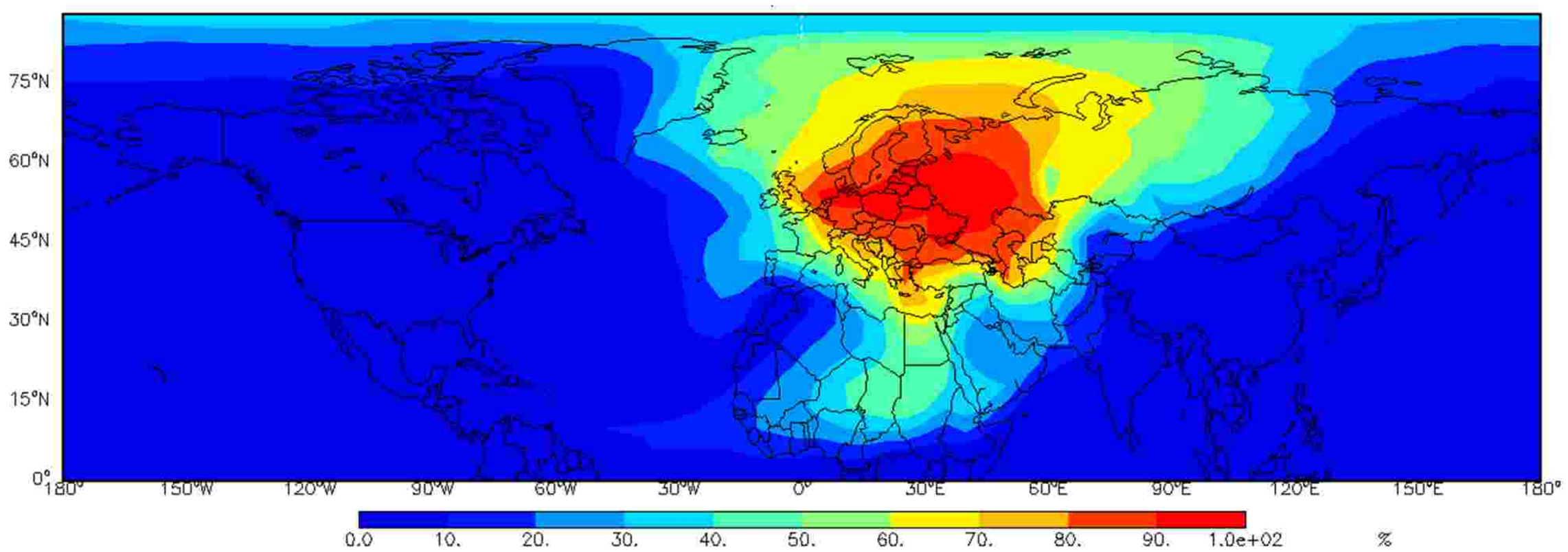
75°N
60°N
45°N
30°N
15°N
0°
180°
150°W
120°W
90°W
60°W
30°W
0°
30°E
60°E
90°E
120°E
150°E
180°
0.0
10.
20.
30.
40.
50.
60.
70.
80.
90.
1.0e+02
%

c)

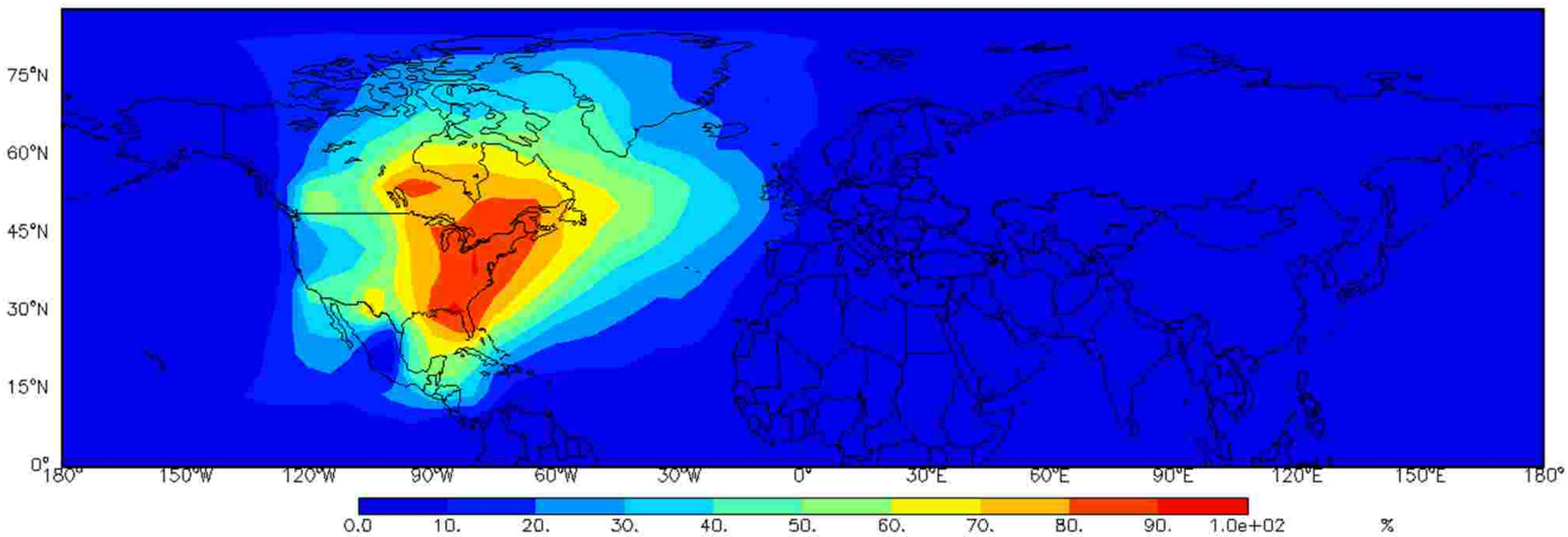
75°N
60°N
45°N
30°N
15°N
0°
180°
150°W
120°W
90°W
60°W
30°W
0°
30°E
60°E
90°E
120°E
150°E
180°
0.0
10.
20.
30.
40.
50.
60.
70.
80.
90.
1.0e+02
%

d)

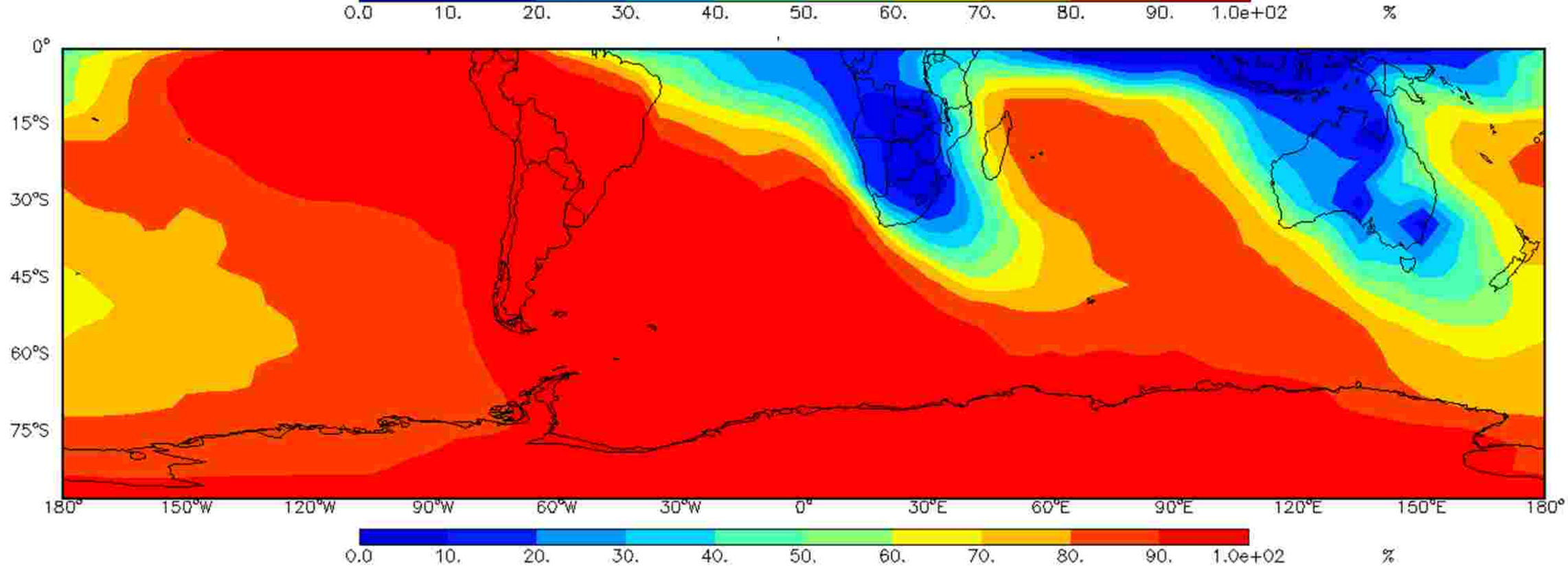
0°
15°S
30°S
45°S
60°S
75°S
180°
150°W
120°W
90°W
60°W
30°W
0°
30°E
60°E
90°E
120°E
150°E
180°
0.0
10.
20.
30.
40.
50.
60.
70.
80.
90.
1.0e+02
%

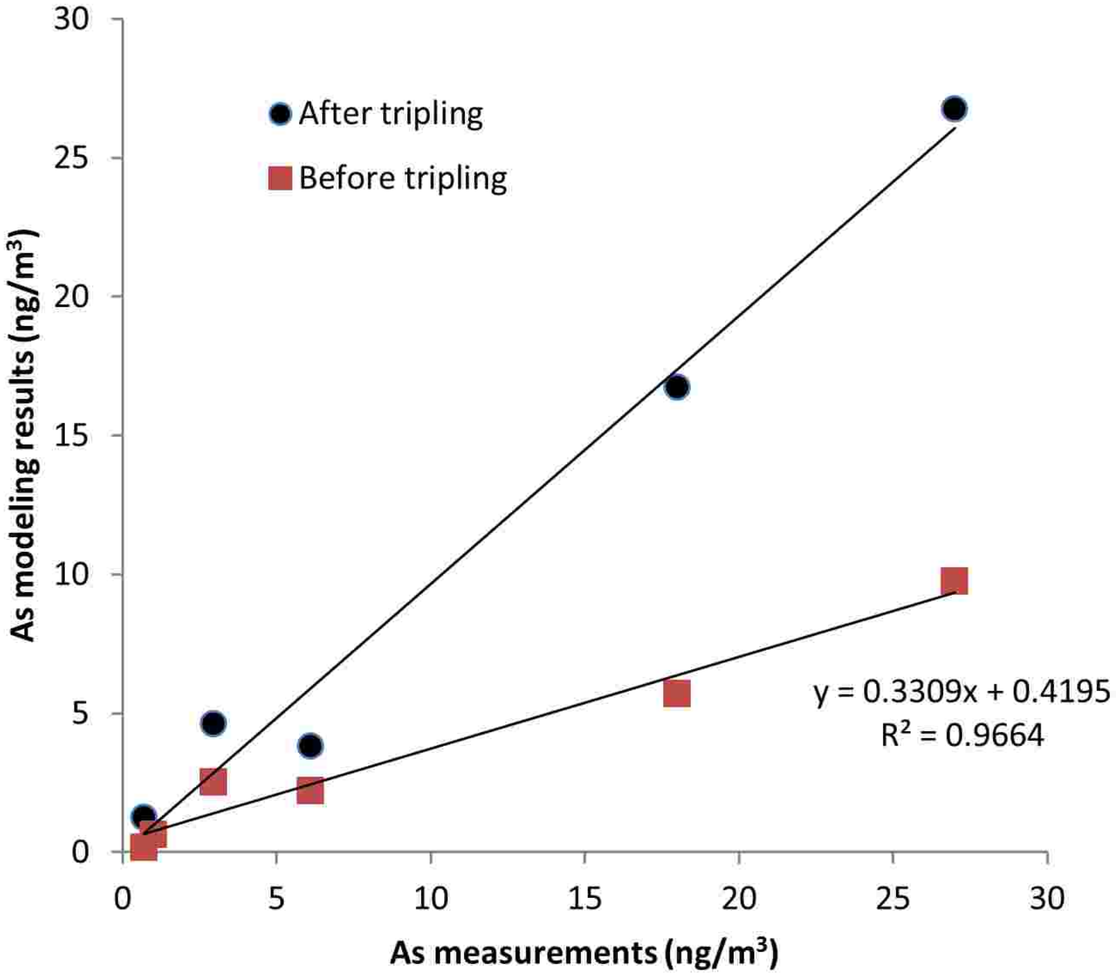
After tripling
Before tripling
As modeling results (ng/m³)
As measurements (ng/m³)
y = 0.3309x + 0.4195
R² = 0.9664
0
5
10
15
20
25
30